Title
Effect of irregularities of nanosatellites position and size on collective electric and magnetic plasmonic resonances in spherical nanoclusters.

Journal
Optics express, 21(6)

ISSN
1094-4087

Authors
Vallecchi, Andrea
Albani, Matteo
Capolino, Filippo

Publication Date
2013-03-25

Effect of irregularities of nanosatellites position and size on collective electric and magnetic plasmonic resonances in spherical nanoclusters

Andrea Vallecchi,[1,*] Matteo Albani,[1] and Filippo Capolino[2]

[1]*Department of Information Engineering, University of Siena, Via Roma 56, 53100 Siena, Italy*
[2]*Department of Electrical Engineering and Computer Science, University of California, Irvine, California 29697, USA*
[*]*andrea.vallecchi@unisi.it*

Abstract: Spherical nanoclusters (NCs) with a central dielectric core surrounded by several satellite plasmonic nanospheres have been recently investigated as aggregates supporting electric and magnetic collective resonances. Notably, the collective magnetic resonance has been exploited to provide magnetic properties in optics, i.e., materials with macroscopic relative permeability different from unity. The NCs discussed in this paper can be realized using state-of-the-art nanochemistry self-assembly techniques. Accordingly, perfectly regular disposition of the nanoplasmonic satellites is not possible and this paper constitutes the first comprehensive analysis of the effect of such irregularities onto the electric and magnetic collective resonances. In particular we will show that the peak of the scattering cross section associated to the magnetic resonance is very sensitive to certain irregularities and significantly less to others. It is shown here that "artificial magnetic" properties of NCs are preserved for certain degrees of irregularities of the nanosatellites positions, however they are strongly affected by irregularities in the plasmonic nanosatellites sizes and by the presence of "defects" caused by the absence of satellites in the process of self-assembly around the dielectric core. The "artificial electric" resonance is instead less affected by irregularities mainly because of its wider frequency bandwidth.

OCIS codes: (160.1245) Artificially engineered materials; (160.3918) Metamaterials; (250.5403) Plasmonics; (240.6680) Surface plasmons; (160.4760) Optical properties.

References and links

1. A. Alù, A. Salandrino, and N. Engheta, "Negative effective permeability and left-handed materials at optical frequencies," Opt. Express **14**(4), 1557–1567 (2006).
2. Y. A. Urzhumov, G. Shvets, J. A. Fan, F. Capasso, D. Brandl, and P. Nordlander, "Plasmonic nanoclusters: a path towards negative-index metafluids," Opt. Express **15**(21), 14129–14145 (2007).
3. C. R. Simovski and S. A. Tretyakov, "Model of isotropic resonant magnetism in the visible range based on core-shell clusters," Phys. Rev. B **79**(4), 045111 (2009).
4. A. Alù and N. Engheta, "The quest for magnetic plasmons at optical frequencies," Opt. Express **17**(7), 5723–5730 (2009).
5. J. A. Fan, C. Wu, K. Bao, J. Bao, R. Bardhan, N. J. Halas, V. N. Manoharan, P. Nordlander, G. Shvets, and F. Capasso, "Self-assembled plasmonic nanoparticle clusters," Science **328**(5982), 1135–1138 (2010).
6. A. Vallecchi, M. Albani, and F. Capolino, "Collective electric and magnetic plasmonic resonances in spherical nanoclusters," Opt. Express **19**(3), 2754–2772 (2011).
7. S. Mühlig, A. Cunningham, S. Scheeler, C. Pacholski, T. Bürgi, C. Rockstuhl, and F. Lederer, "Self-assembled plasmonic core-shell clusters with an isotropic magnetic dipole response in the visible range," ACS Nano **5**(8), 6586–6592 (2011).
8. D. K. Morits and C. R. Simovski, "Negative effective permeability at optical frequencies produced by rings of plasmonic dimers," Phys. Rev. B **81**(20), 205112 (2010).
9. D. Morits and C. Simovski, "Isotropic negative effective permeability in the visible range produced by clusters of plasmonic triangular nanoprisms," Metamaterials (Amst.) **5**(3), 71–78 (2011).
10. S. Zhang, D. A. Genov, Y. Wang, M. Liu, and X. Zhang, "Plasmon-induced transparency in metamaterials," Phys. Rev. Lett. **101**(4), 047401 (2008).

#182380 - $15.00 USD Received 27 Dec 2012; accepted 5 Feb 2013; published 21 Mar 2013

11. U. Fano, "Effects of configuration interaction on intensities and phase shifts," Phys. Rev. **124**(6), 1866–1878 (1961).
12. J. A. Fan, K. Bao, C. Wu, J. Bao, R. Bardhan, N. J. Halas, V. N. Manoharan, G. Shvets, P. Nordlander, and F. Capasso, "Fano-like interference in self-assembled plasmonic quadrumer clusters," Nano Lett. **10**(11), 4680–4685 (2010).
13. S. N. Sheikholeslami, A. García-Etxarri, and J. A. Dionne, "Controlling the interplay of electric and magnetic modes via Fano-like plasmon resonances," Nano Lett. **11**(9), 3927–3934 (2011).
14. C. F. Bohren and D. R. Huffman, *Absorption and Scattering of Light by Small Particles* (Wiley, 1983).
15. S. Steshenko and F. Capolino, "Single dipole approximation for modeling collections of nanoscatterers" in *Theory and Phenomena of Metamaterials*, F. Capolino, ed. (CRC, 2009), Chap. 8.
16. P. C. Waterman and N. E. Pedersen, "Electromagnetic scattering by periodic arrays of particles," J. Appl. Phys. **59**(8), 2609 (1986).
17. V. Ponsinet, A. Aradian, P. Barois, and S. Ravaine, "Self-assembly and nanochemistry techniques towards the fabrication of metamaterials," in *Applications of Metamaterials*, F. Capolino, ed. (CRC, 2009), Chap. 32.
18. J. Dintinger, S. Mühlig, C. Rockstuhl, and T. Scharf, "A bottom-up approach to fabricate optical metamaterials by self-assembled metallic nanoparticles," Opt. Mater. Express **2**(3), 269–278 (2012).
19. C. Helgert, C. Rockstuhl, C. Etrich, C. Menzel, E.-B. Kley, A. Tünnermann, A. F. Lederer, and T. Pertsch, "Effective properties of amorphous metamaterials," Phys. Rev. B **79**(23), 233107 (2009).
20. B. W. Clare and D. L. Kepert, "The closest packing of equal circles on a sphere," Proc. R. Soc. Lond. A Math. Phys. Sci. **405**(1829), 329–344 (1986).
21. J. E. Hansen, *Spherical Near-Field Antenna Measurements* (Peter Peregrinus Ltd., 1988).
22. W. Cai and V. Shalaev, *Optical Metamaterials: Fundamentals and Applications* (Springer, 2010).

1. Introduction

Clusters of self-assembled plasmonic nanoparticles can be used as building blocks for new magnetic or negative index materials at optical frequencies [1–7]. In particular, nanoclusters (NCs) of spherical shape formed by a number of satellites made of silver nanocolloids, each enclosed within a thin dielectric shell, and all attached to a dielectric core of variable size can provide isotropic electric and magnetic resonances in three-dimensions (3D) [6]. NCs with satellites of different shapes, like dimers and triangular nanoprisms, have been also proposed [8,9]. Indeed, in this type of structures the plasmonic particles are arranged to force the electric field to circulate in the plane orthogonal to the incident magnetic field, inducing an overall collective "magnetic resonance" that may coexist with the individual electric resonance supported by each constituent nanoparticle. The magnetic resonance mode is sometimes referred to as a "dark mode" because it weakly couples to external fields, or weakly scatters, and has great relevance in the electromagnetic induced transparency (EIT) phenomenon [10] and Fano-like resonances [11–13]. The weak scattering of this dark mode implies that the magnetic resonance is a narrow band phenomenon, contrarily to the electric mode. Arrangements of spherical NCs as shown in this paper are a viable solution for future composite materials or fluids with magnetic properties at optical frequencies.

An effective approach to theoretically model the optical response of spherical NC metamaterials has been described in [6]. This approach is based on the application of the single dipole approximation (SDA) [14,15] for each NC satellite, in conjunction with the multipole expansion of the NC scattered field to evaluate the electric and magnetic polarizabilities of an isolated NC.

It has been shown in [6] that NCs made of plasmonic nanosatellites support *collective plasmon modes* among which the most relevant are those associated with the induced electric and magnetic NC-dipole resonances, that can be tuned by varying the number of nanosatellites, their separation, and the permittivity of the host material. Furthermore, in [6] the effective permittivity and permeability of the composite media formed by periodical arrangements of NCs have been estimated by an extension of the Maxwell Garnett homogenization model including higher order multipole interactions among nanoparticles in the quasistatic and infinitesimal lattice limits [16]. Within these approximations, it was found that metamaterials made of close-packed arrangements of NCs exhibit resonant responses of the permittivity and permeability that can both reach negative values at frequencies right above the respective resonances. Moreover, the electric and magnetic resonance positions can be tuned by engineering the constituent NC configuration to achieve sufficient overlapping

#182380 - $15.00 USD Received 27 Dec 2012; accepted 5 Feb 2013; published 21 Mar 2013

between the negative permittivity and negative permeability regions so as to simultaneously have $\mathrm{Re}(\varepsilon_r^{eff}) < 0$ and $\mathrm{Re}(\mu_r^{eff}) < 0$, and thus a negative index in the optical range.

NC metamaterials can be effectively fabricated by nanochemistry and self-assembly techniques [17,18]. In [6] we have initially assumed for simplicity that NCs can be realized according to a regular distribution and size of metal nanoparticles around the dielectric core, and then assembled as a perfect crystal. However, the fabrication of regular NCs is unlikely to be achieved with bottom-up methods, and in practice there exists some disorder degree. It is therefore of interest to estimate the effect of such kinds of disorder on the optical properties of NCs. Namely, both the effect of dimensional and positional disorders as well as of the presence of defects within a NC, that take place because particles can physically block one another in the process of self-assembly around the core, have been analysed. The aim is to select those structures which exhibit larger artificial magnetism and the response of which is more insensitive to the presence of irregularities in the NC configuration. Moreover, self-assembling systems can be controlled to create specific periodic nanostructured patterns with long-range order of the domains. Nonetheless, the arrays of microdomains typically still contains some uncontrolled defects and usually lacks global registration and orientation. Accordingly it is also important to characterize how these larger scale structural disorder effects are related with variations and degradation in the optical properties of self-assembled metamaterials, and whether the electric and magnetic responses predicted for completely regular arrangements will be retained. Indeed, the assignment of effective properties to such disordered metamaterials constitutes a challenging task. It can potentially be achieved by analyzing the scattering properties of individual scattering inclusions in terms of electromagnetic multipole contributions and successive incorporation of the actual dipole moments into averaging procedures that do not require regular spatial arrangement [19]. However, the characterization of disordered assemblies of NCs is beyond the scope of the present investigation.

In this work the optical response of 3D NCs are studied by Monte Carlo simulations. Different types of structural deviations from the perfect arrangement are considered, namely, variable constituent particle sizes (Sec. 3), irregular disposition of the particle around the core (Sec. 4), and the presence of defects (Sec. 5). We show that while displacement of particles from their nominal positions has negligible effect on the magnetic response of NCs, increasingly larger variability of particle sizes, as well as absence of satellites, progressively reduces the intensity of the average electric and magnetic responses and may determine offset of the resonance frequencies.

2. Modeling of disordered nanoclusters

NCs are formed by evenly distributing a number of colloidal metal nanoparticles around a dielectric (silica, SiO_2) core in a way to obtain a compact and regular ensemble minimizing anisotropy and spatial dispersion effects. The maximum number of nanoparticles that can be clustered around the central silica core is related to their size. Depending on the chosen number of nanoparticles, for the purpose of modelling their nominal positions around the silica core can be assigned either by an analytical distribution law (regular NCs), assuming for example that they coincide with the vertices of a Platonic solid, or through a numerical procedure (pseudo-regular NCs) based on the maximization of the minimum interparticle distance [6,20]. Both approaches used to theoretically define the positions of nanosatellites lead to uniform (or pseudouniform) distributions of the nanosatellites around the central dielectric core, contributing to the desired isotropy of the NC optical response.

The different types of NC irregularities considered are schematically illustrated in Fig. 1. Uncorrelated dimensional and positional disorder is introduced into the nominal NC system (Fig. 1(a)) either by adding to the nominal particle size a uniformly distributed perturbation randomly chosen within a given interval (Fig. 1(b)), or displacing each nanoparticle from its original position on a spherical coordinate grid by adding a uniformly distributed spatial disorder (Fig. 1(c)). To avoid overlapping of nanoparticles due to the nonuniform sizes and

#182380 - $15.00 USD Received 27 Dec 2012; accepted 5 Feb 2013; published 21 Mar 2013

position uncertainty, the largest variations are assumed to be smaller than the minimum separation between nanoparticles in the nominal configuration. Furthermore, defective NC configurations are simply obtained by removing from the nominal NCs a certain number of nanoparticles at random (possibly adjacent) locations (Fig. 1(d)).

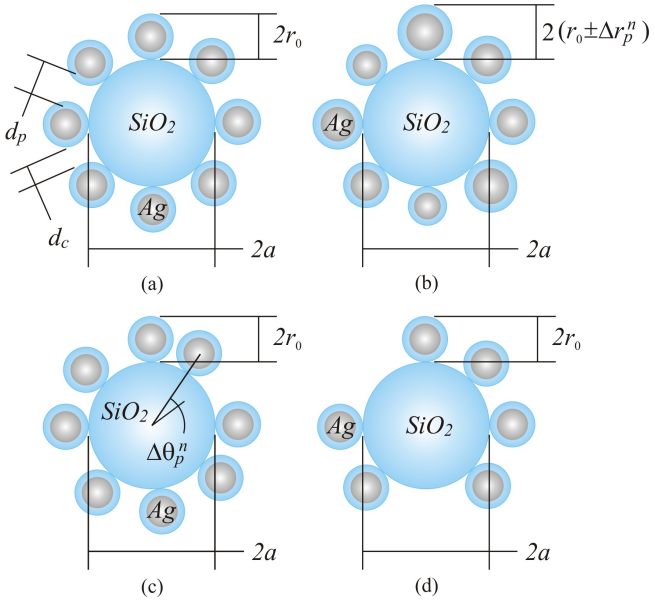

Fig. 1. Types of irregularities that can occur in 3D spherical NCs realized by self-assembly techniques: (a) theoretical perfectly regular arrangement, (b) variable sizes of nanosatellites, (c) displacement of nanosatellites with respect to nominal positions, and (d) presence of nanosatellites defects.

The effects of *dimensional* (Sec. 3) and *positional* (Sec. 4) disorders and of the presence of *defects* (Sec. 5) are investigated separately. To characterize the optical response of NCs, and particularly their magnetic properties, we follow the approach outlined in [6]. An approximate model based on the SDA [6,14,15] is used to determine the field scattered by a NC under plane wave illumination. The scattered field is then expanded into spherical harmonics and the various equivalent multipoles of the NC are derived [21]. The frequency position and strength of the NCs resonances are identified through the analysis of the extinction, scattering, and absorption efficiencies. The nature of the various NC resonances is recognized by decomposing the total scattering efficiency $Q_{sca} = C_{sca} / C_{geom}$, where C_{sca} is the scattering cross section and $C_{geom} = \pi(\mathrm{D}/2)^2$ is the geometrical cross section of the minimal sphere enveloping the cluster [6,14], into the efficiency contributions originated by the induced electric and magnetic dipole moments, $Q_{sca}^{p_e}$ and $Q_{sca}^{p_m}$ respectively, and that associated with all the remaining higher order multipoles Q_{sca}^{mps}, which are plotted separately; i.e., $Q_{sca} = Q_{sca}^{p_e} + Q_{sca}^{p_m} + Q_{sca}^{mps}$. The electric and magnetic resonance frequencies will correspond to the peaks of $Q_{sca}^{p_e}$ and $Q_{sca}^{p_m}$, respectively. By this approach, the individual scattering responses of a population of NCs, large enough to ensure statistical significance, are computed and results are finally aggregated and the effects of disorder on the electric and magnetic properties of NCs are characterized statistically in terms of probability density functions (pdfs). The obtained statistical average is also representative of a volume average involved in effective homogenized parameter retrieval for a metamaterial made by a collection of NCs that are only nominally identical, but in practice all different, because of randomness in the realization process.

#182380 - $15.00 USD Received 27 Dec 2012; accepted 5 Feb 2013; published 21 Mar 2013

The NC satellites are assumed to be made of silver whose permittivity is described with the following size dependent Drude model [22]

$$\varepsilon_m = \varepsilon_\infty - \frac{\omega_p^2}{\omega\left[\omega + i\Gamma\left(r_p\right)\right]} \tag{1}$$

where ε_∞ is the background permittivity of the metal, ω_p and Γ are the plasma and damping radian frequencies, and r_p denotes the plasmonic nanosphere radius. The size dependent damping frequency incorporated into the Drude model takes into account the alteration in the mean free path of the conduction electrons which arises when the size of the nanosatellites approaches the bulk mean free path length, and the movement of free electrons is further limited by the physical boundary of the metal structure, and can be expressed as

$$\Gamma\left(r_p\right) = \Gamma_\infty + A\frac{v_F}{r_p}. \tag{2}$$

Here Γ_∞ is the damping constant of bulk silver, A is a constant term assumed to be approximately unity, i.e. $A = 1$, and v_F is the Fermi velocity. Specifically, the Drude parameters and the Fermi velocity values used for silver in our simulations across the optical range are: $\varepsilon_\infty = 5$, $\omega_p = 1.37\times10^{16}$ rad/s, $\Gamma_\infty = 27.3\times10^{12}$ rad/s, $v_F = 1.39\times10^6$ m/s.

For simplifying the analysis, similarly to [2], we assume that the host medium and the dielectric core, as well as the dielectric coating of nanospheres required to avoid strong near-field coupling of neighbouring colloids affecting individual particle resonance and causing inhomogeneous spectral-line broadening, have the same permittivity $\varepsilon_r = 2.2$. Indeed, our model well approximates the case of a glass core, and all clusters immersed in a solvent with such or similar permittivity.

3. Effect of irregularity of nanosatellites dimensions on nanocluster response

We introduce uncorrelated dimensional disorder into a NC by assuming that the size of each constituent nanoparticle is randomly variable within a given range. Specifically, if the NC comprises N nanosatellites, their radii r_p will be represented by a vector of uncorrelated pseudorandom numbers generated with uniform distribution

$$\left[r_p\right] = \left(r_0 - \Delta r_p\right) + 2\Delta r_p \,\mathrm{rand}(N) \tag{3}$$

where r_0 is the nominal particle size, Δr_p is the maximum particle size variation, and $\mathrm{rand}(N)$ denotes a vector of N random numbers distributed uniformly in [0,1] (see Fig. 1(b)). According to Eq. (3), radii of nanoparticles vary in the range $[r_0 - \Delta r_p, r_0 + \Delta r_p]$. The distance of each nanoparticle from the NC centre is adjusted depending on the particle size so that each nanoparticle surface is lying right outside the central dielectric core. Interparticle distance in the original regular NC configuration, before randomization of particle sizes, is chosen to avoid any particle overlapping that could occur because of randomization of particle sizes. By this approach we generate a population of NCs and we compute their individual scattering responses. Scattering efficiencies when each NC is illuminated by a linearly polarized plane wave are computed as in [6] to characterize the frequency position and strength of the NCs resonances. Results are finally aggregated statistically.

In the following we examine the effect of dimensional disorder on the performance of different types of NCs for a given maximum particle size variation Δr_p. In particular, four NC types are analyzed, comprising 4, 12, 32, and 48 spherical plasmonic nanosatellites.

#182380 - $15.00 USD Received 27 Dec 2012; accepted 5 Feb 2013; published 21 Mar 2013

3.1 NC made of 4 plasmonic nanosatellites

As the first example, we refer to a regular tetrahedral NC configuration made of 4 solid silver nanospheres of nominal radius $r_0 = 20$ nm, arranged around a central dielectric core of radius $a = 9.8$ nm, with overall diameter of the NC equal to $D = 108$ nm. The surface-to-surface interparticle distance in this reference NC configuration is set to $d_p = 12$ nm. It is made provision for a 2-nm-thick coating of the metal particles with polymer shells, and to avoid any particle overlapping maximum deviation of particle size from its nominal value is assumed to be smaller than the remaining distance between the coated spheres ($d_c = 8$ nm). In particular, we assume to have a maximum particle size variation $\Delta r_p = 4$ nm. Figure 2(a) shows one of the NC configurations from the generated population of 100 samples with random particle sizes. The histogram plotted in Fig. 2(b) confirms that particle size distribution is substantially uniform over the range $[r_0 - \Delta r_p, r_0 + \Delta r_p]$.

After simulation by the SDA and multipole expansion of the scattered fields for each NC of the population, results for the dipolar and higher order multipole scattering efficiencies have been aggregated into the statistics shown in Fig. 3. Indeed, the statistical significance of these data was established by simulation of a larger population of NCs, whose results showed negligible deviations from those obtained for the 100 NC population. In Fig. 3, besides the magnetic dipolar scattering efficiency, we also report the electric dipole and higher order multipole scattering efficiencies against frequency. To achieve a comprehensive characterization of the fluctuations in the strength and position of the NC resonances induced by the variability of particle size, in Fig. 3 we show the 5, 50, and 95 percentile curves (dashed lines) along with the corresponding empirically estimated pdf of the scattering efficiencies (color shaded stripes behind plotted curves). Namely, we have calculated the pdf of $\log_{10} Q_{sca}^{p_e, p_m, mps}$, the value of which is proportional to the respective color intensity according to the gray shaded colorbar. Scattering efficiencies for the nominal tetrahedral NC configuration are also plotted (continuous lines), as a reference for the purpose of comparison.

It can be observed that for the considered maximum deviation of particle size from the nominal value, corresponding to 20% of the nominal particle size r_0, in this particular case all the NC collective resonances occur at approximately the same frequencies as in the reference NC. However, resonance bandwidths enlarge due to the detuning of individual satellite resonances which also smoothes down the average intensities of resonances. Moreover, the variances of the scattering efficiencies, which are proportional to the width of the pdf color stripes or, equivalently, to the inter-percentile range, are rather pronounced, and their medians (50 percentiles) tend to the corresponding (nominal) reference curves, especially near resonant frequencies.

The NC exhibits electric and magnetic resonances at close frequencies, around 632 THz and 636 THz, respectively. A higher order multipole is also strongly excited around 692 THz. It is noted that the spread of the magnetic dipole scattering efficiency $Q_{sca}^{p_m}$ is larger than that of the electric dipole scattering efficiency $Q_{sca}^{p_e}$, which is likely due to the fact that the magnetic resonance depends both on the size of the equivalent loop formed by currents circulating around the central dielectric core of the cluster and the dimensions of the individual particles forming this loop, whereas the electric dipole resonance mainly depends on these latter. Analogously, the average strength of the magnetic dipole resonance (the peak of $Q_{sca}^{p_m}$) is reduced more noticeably than that of the electric dipole.

#182380 - $15.00 USD Received 27 Dec 2012; accepted 5 Feb 2013; published 21 Mar 2013

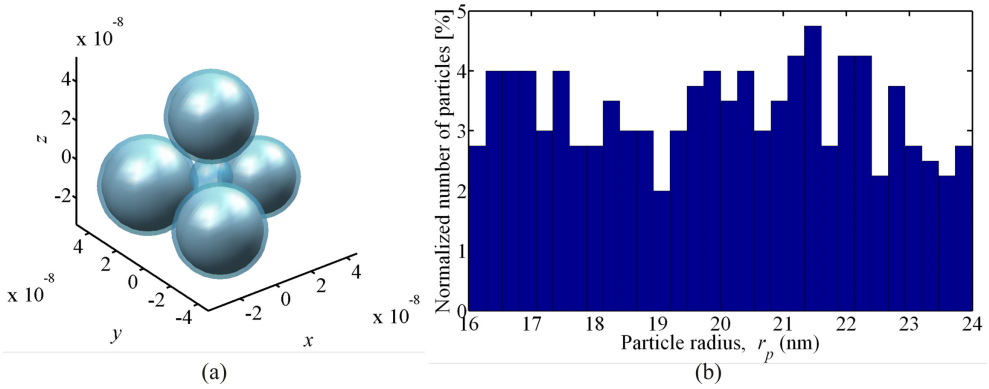

Fig. 2. (a) Sample tetrahedral NC with randomly variable particle size ($r_0 = 20$, $\Delta r_p = 4$ nm). (b) Particle size distribution for the simulated population of 100 NCs.

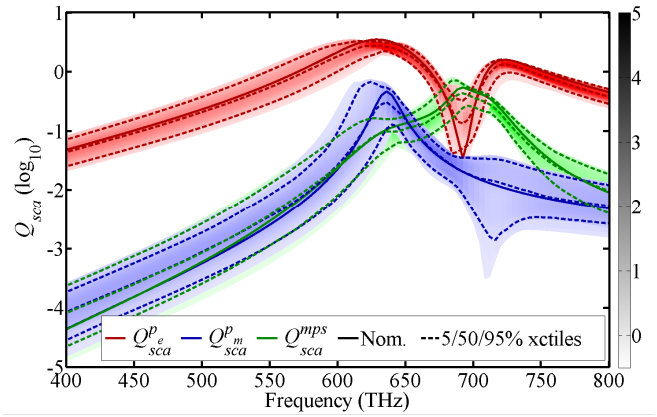

Fig. 3. Statistics of the scattering efficiency contributions associated with the induced electric and magnetic dipole moments and the remaining higher order multipoles for the population of 100 tetrahedral NCs with $r_0 = 20$ nm and for $\Delta r_p = 4$ nm from Fig. 2. The 5, 50, and 95 percentile curves are superimposed to the relative empirical pdfs (color shaded stripes).

3.2 NC made of 12 plasmonic nanosatellites

Next, we examine the effects of dimensional disorder in an icosahedral NC made of 12 solid silver nanospheres of nominal radius $r_0 = 15$ nm arranged around a central dielectric particle of radius $a = 21$ nm, with overall size of the NC equal to $D = 110$ nm. The surface-to-surface distance between two nanosatellites in the nominal NC configuration is fixed to $d_p = 10$ nm and we assume in Eq. (3) a maximum particle size variation $\Delta r_p = 3$ nm (i.e., 20% of the nominal particle size r_0 as in the tetrahedral NC previously considered). Through the random process described by Eq. (3), we generate a population of 100 NCs, of the type shown in Fig. 4(a), that exhibit the distribution of particle sizes illustrated by the histogram in Fig. 4(b), which is substantially uniform over the range $[r_0 - \Delta r_p, r_0 + \Delta r_p]$. Dispersion of scattering efficiencies plotted in Fig. 5 is in the order of that observed for the population of tetrahedral NCs examined in the preceding example, and indeed for these two sets of experiments the relative maximum deviation of particle size from the nominal value is the same ($\Delta r_p / r_0 = 0.2$).The NCs exhibit a magnetic resonance around 605 THz and an electric resonance around 660 THz. A higher order multipole is also strongly excited around 660 THz

#182380 - $15.00 USD
Received 27 Dec 2012; accepted 5 Feb 2013; published 21 Mar 2013

and 750 THz. As observed for the tetrahedral case, the average magnetic dipole resonance strength (the peak of $Q_{sca}^{p_m}$) is reduced more noticeably than that of the electric dipole.

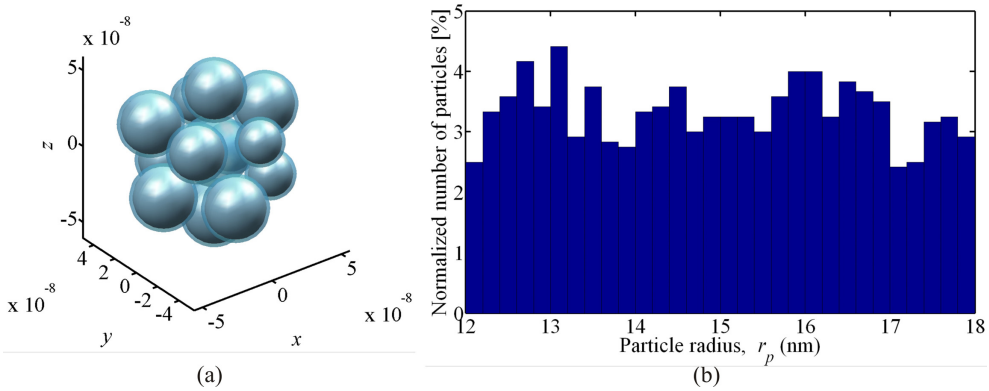

Fig. 4. (a) Sample icosahedral NC with randomly variable particle size ($r_0 = 15$, $\Delta r_p = 3$ nm). (b) Particle size distribution for the simulated population of 100 NCs.

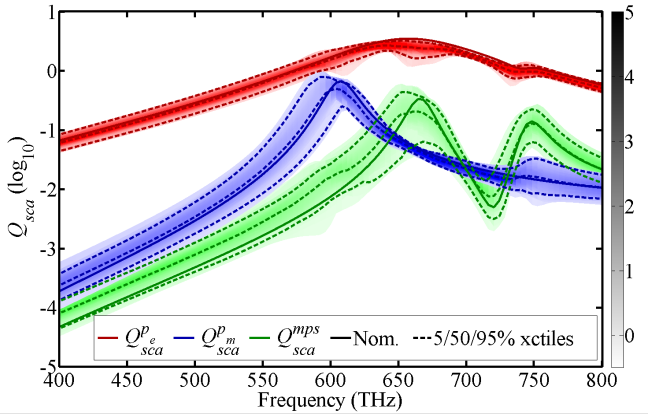

Fig. 5. Statistics of the scattering efficiency contributions associated with the induced electric and magnetic dipole moments and the remaining higher order multipoles for the population of 100 icosahedral NCs with $r_0 = 15$ nm and for $\Delta r_p = 3$ nm from Fig. 4. The 5, 50, and 95 percentile curves are superimposed to the relative empirical pdfs (color shaded stripes).

3.3 NC made of 32 plasmonic nanosatellites

As another example relative to the effect of particle size disorder, we consider a NC made of 32 solid silver nanospheres with nominal radius of 10 nm arranged around a central dielectric core of radius $a = 31.7$ nm, with overall size of the NC $D = 111.4$ nm. Sizes of nanosatellites is not uniform and is assumed again to have a pseudorandom uniform distribution given by Eq. (3) with $\Delta r_p = 2$ nm. The surface-to-surface distance between two nanoparticles in the nominal NC configuration is set to $d_p = 8$ nm to avoid any particle overlapping in the model in the presence of 2-nm-thick polymer shells coating the metal nanosatellites (i.e., $d_c = 4$ nm).

We have generated a population of 100 NCs, an instance of which is exemplified in Fig. 6(a). The distribution of particle size for the NC population is randomly variable with substantially uniform distribution in the range $[r_0 - \Delta r_p, r_0 + \Delta r_p]$, as apparent from the

#182380 - $15.00 USD Received 27 Dec 2012; accepted 5 Feb 2013; published 21 Mar 2013

histogram plotted in Fig. 6(b). The statistics for the simulated scattering efficiencies of the considered NC population against frequency are shown in Fig. 7. NC collective resonances appear to occur at approximately the same frequencies as in the original nominal particle size NC, but detuning of individual satellite resonances provides some enlargement of resonance bandwidths while resonance strengths are decreased, especially for the magnetic dipole resonance (the peak of $Q_{sca}^{p_m}$). Fluctuations of the electric and magnetic responses across the NC population induced by the variability of particle size can also be observed. However, the impact of particle size randomness on the optical response of this type of NCs is generally less severe than in the populations of tetrahedral and icosahedral NCs previously analyzed, though the relative maximum deviation of particle size from the nominal value $\Delta r_p / r_0$ is the same for all these populations. The main reason why the magnetic resonance is more sensitive to statistical variations relies on the higher quality factor of its resonance, caused by lower radiation losses than in the electric one.

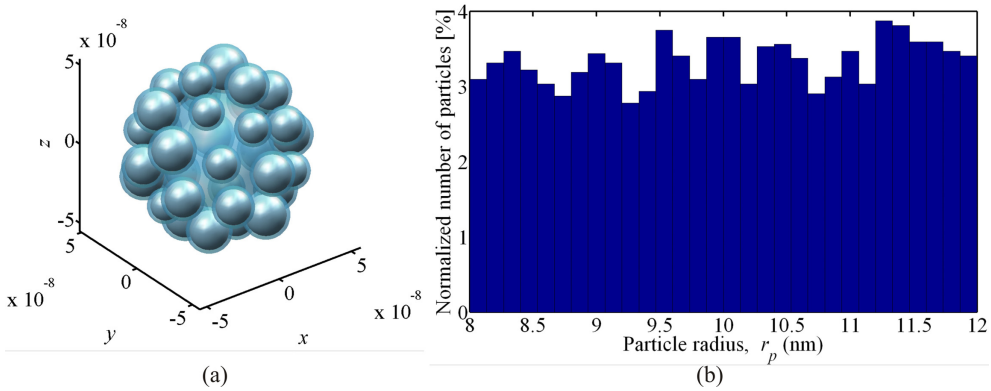

Fig. 6. (a) Sample 32-element NC with randomly variable particle size ($r_0 = 10$, $\Delta r_p = 2$ nm). (b) Particle size distribution for the simulated population of 100 NCs.

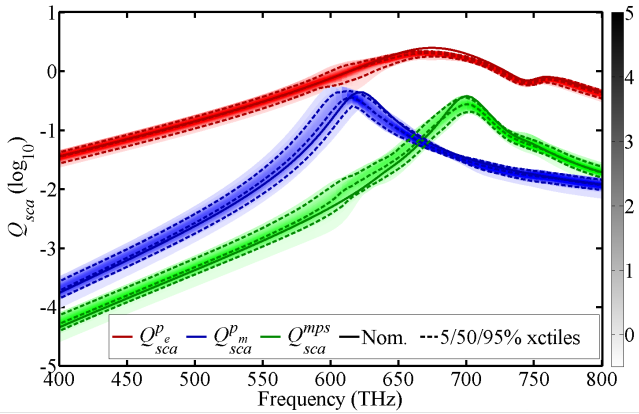

Fig. 7. Statistics of the scattering efficiency contributions associated with the induced electric and magnetic dipole moments and the remaining higher order multipoles for the population of 32-nanosatellites NCs with $r_0 = 10$ nm and for $\Delta r_p = 2$ nm from Fig. 6. The 5, 50, and 95 percentile curves are superimposed to the relative empirical pdfs (color shaded stripes).

3.4 NC made of 48 plasmonic nanosatellites

The above results suggest that NCs comprising a larger number of particles can be more insensitive to the effects of disorder. To confirm this trend, as the last example relative to the

#182380 - $15.00 USD Received 27 Dec 2012; accepted 5 Feb 2013; published 21 Mar 2013

effect of particle size disorder, we have considered a NC formed by 48 solid silver nanospheres of nominal radius $r_0 = 8.5$ nm attached to a central core of radius $a = 35.5$ nm, with overall size of the NC equal to $D = 113$ nm. Particle size is assumed to be not uniform and to have a pseudorandom uniform distribution with maximum particle size variation $\Delta r_p = 1.7$ nm. The surface-to-surface distance between two nanoparticles in the nominal NC configuration is fixed to $d_p = 7.4$ nm to avoid any overlapping of metal nanoparticles that are assumed to be coated with 2-nm-thick polymer shells (i.e., $d_c = 3.4$ nm).

In Fig. 8(a) is shown an instance of the 100 NCs population we have generated by the random process (3). The distribution of particle size for the NC population is randomly variable with substantially uniform distribution in the range $[r_0 - \Delta r_p, r_0 + \Delta r_p]$, as illustrated in the histogram plotted in Fig. 8(b). The statistics for the simulated scattering efficiencies of the considered NC population against frequency are shown in Fig. 9. Similarly to the previous example of the 32-element NCs, fluctuations of the electric and magnetic responses across the NC population induced by the variability of particle size is limited, though still the spread of the magnetic dipole scattering efficiency $Q_{sca}^{p_m}$ is slightly larger than that of the electric one. At any rate, the impact of particle size randomness on the optical response of this type of NCs appears to be weaker than in the populations of tetrahedral and icosahedral NCs with the same relative maximum deviation $\Delta r_p / r_0 = 0.2$ of particle size.

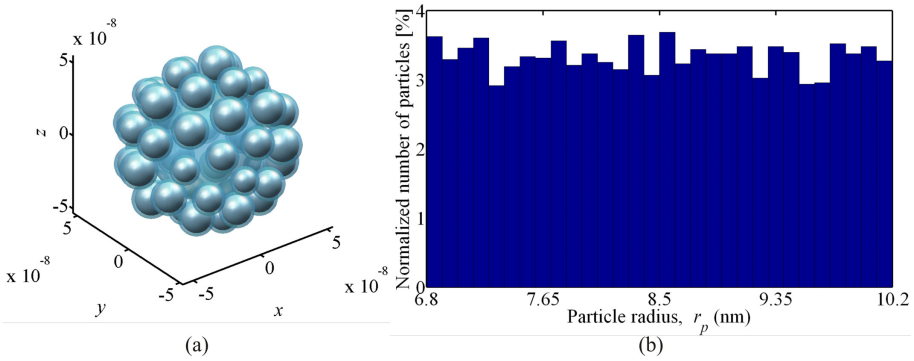

(a) (b)

Fig. 8. (a) Sample 48-element NC with randomly variable particle size ($r_0 = 8.5$, $\Delta r_p = 1.7$ nm). (b) Particle size distribution for the simulated population of 100 NCs.

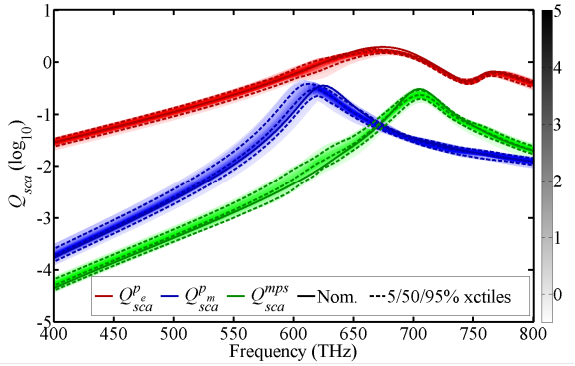

Fig. 9. Statistics of the scattering efficiency contributions associated with the induced electric and magnetic dipole moments and the remaining higher order multipoles for the population of 48-nanosatellites NCs with $r_0 = 8.5$ nm and for $\Delta r_p = 1.7$ nm from Fig. 8. The 5, 50, and 95 percentile curves are superimposed to the relative empirical pdfs (color shaded stripes).

#182380 - $15.00 USD
Received 27 Dec 2012; accepted 5 Feb 2013; published 21 Mar 2013

The downside for the increased robustness and substantial immunity to irregularity of nanosatellites dimensions exhibited by the NCs comprising a larger number of nanosatellites is a possible reduction of the electric and magnetic response intensities, as a consequence of the increased absorption occurring in the smaller size nanosatellites. This is duly taken into account by the size dependent damping frequency (2) incorporated into the Drude model of silver (1) we have used in our simulations. However, our results show that for the 48-element NCs the reduction of scattering efficiencies due to damping losses is marginal. Furthermore, though the magnetic resonance is always more affected than the electric one, it is very important to note that a clear and strong peak of the magnetic resonance is still present.

4. Effect of irregularity of nanosatellites positions on nanocluster response

To study the effects of an irregular arrangement of nanosatellites, we introduce positional disorder into a NC by assuming that positions of constituent nanoparticles are randomly variable with respect to the nominal values within a given spatial range. Specifically, while sizes of satellites is kept uniform (r_0), their positions are perturbed assuming uncorrelated pseudorandom uniform distributions for elevation and azimuth angular deviations with respect to the axis passing through the NC centre and the original centre position of each nanosatellite

$$\left[\Delta\theta_p\right] = \frac{\left[\Delta R_p\right]}{\left(r_0 + a + t_c\right)} = \frac{\Delta R\,\mathrm{rand}(N)}{\left(r_0 + a + t_c\right)}; \quad \left[\Delta\phi_p\right] = 2\pi\,\mathrm{rand}(N) \tag{4}$$

where a is the radius of the NC core, t_c is the thickness of particle coating, ΔR is the maximum particle displacement, and $\mathrm{rand}(N)$ denotes a vector of N random numbers distributed uniformly in [0,1], where N is the number of nanosatellites forming the considered NC. According to Eq. (4), nanoparticles are randomly displaced within a spherical cap of radius ΔR centred in the nominal nanosatellites positions.

Since nanoparticle size is kept uniform, distance of nanoparticles from the NC centre is unchanged. Interparticle distance in the nominal NC configuration is chosen to avoid any particle overlapping that could occur because of variability of particle position.

Following the same approach used to characterize the sensitivity of the NC optical response to particle size disorder, after generating a population of NCs with randomly displaced nanoparticle positions, we compute by the SDA their individual scattering responses for illumination by a linearly polarized plane wave. Results are then aggregated to statistically characterize the effect of positional disorder on the optical properties of different types of NCs for a given maximum particle position displacement ΔR .

We refer to the same nominal NC configurations considered in the previous section, that is the tetrahedral, icosahedral, 32- and 48-element NCs, with the same nominal geometrical dimensions of the metallic nanoparticles and dielectric core as specified above. For all the types of NCs, we generate a population of 100 sample configurations, that, as mentioned above, is large enough to ensure statistical significance of simulated data.

4.1 NC made of 4 plasmonic nanosatellites

In Fig. 10 and Fig. 11 are shown the results for the tetrahedral NC (with nanosatellite radius of 20 nm, central dielectric core radius $a = 9.8$ nm, overall size of the cluster $D = 108$ nm, and surface-to-surface distance between two nanosatellites in the nominal NC configuration set to $d_p = 12$ nm). In this case we have assumed a maximum displacement of nanosatellites from their nominal positions equal to $\Delta R = 4$ nm. Figure 10(a) shows a sample tetrahedral NC from the generated population with random particle positions, while in Fig. 10(b) is plotted the distribution of nanoparticle displacement distances from their nominal positions for the simulated NC population.

#182380 - $15.00 USD Received 27 Dec 2012; accepted 5 Feb 2013; published 21 Mar 2013

The statistics for the simulated scattering efficiencies of the considered tetrahedral NC population against frequency are shown in Fig. 11. The effect of positional disorder on the optical response of tetrahedral NCs appears to be limited and less significant than that of particle size disorder. The magnetic resonance (the peak of $Q_{sca}^{p_m}$) is stable with respect the statistical variations of nanosphere positions, despite the very low number of nanosatellites.

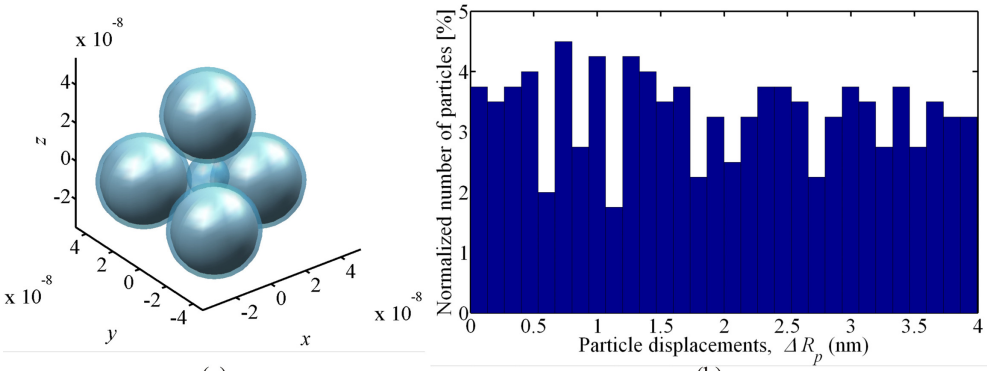

(a) (b)

Fig. 10. (a) Sample tetrahedral NC with randomly variable particle positions ($r_0 = 20$, $\Delta R = 4$ nm). (b) Distribution of nanoparticle displacement distances from their nominal positions for the simulated population of 100 NCs.

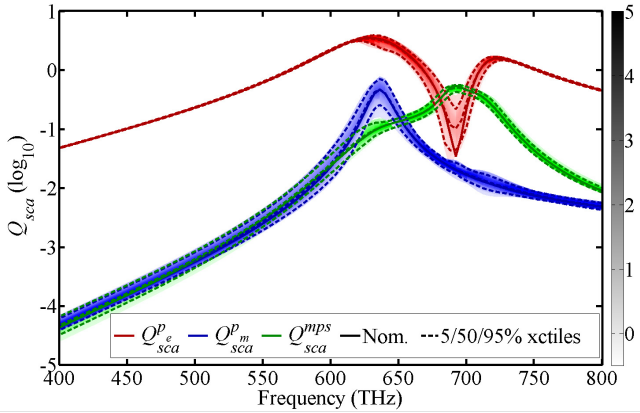

Fig. 11. Statistics of the scattering efficiency contributions associated with the induced electric and magnetic dipole moments and the remaining higher order multipoles for the population of 100 tetrahedral NCs with $r_0 = 20$ nm and variable nanosatellites positions ($\Delta R = 4$) nm from Fig. 10. The 5, 50, and 95 percentile curves are superimposed to the relative empirical pdfs (color shaded stripes).

4.2 NC made of 12 plasmonic nanosatellites

For the icosahedral NC we have assumed the maximum displacement of nanosatellites from their nominal positions to be $\Delta R = 3$ nm (i.e., 20% of particle size). The nanosatellite radius is $r_0 = 15$ nm and the overall size of the NC is $D = 110$ nm. The surface-to-surface distance in the regular NC configuration is set to $d_p = 10$ nm. An instance of the icosahedral NC population with random particle positions is exemplified in Fig. 12(a). The histogram in Fig. 12(b) shows the distribution of nanoparticle displacement distances from their nominal

#182380 - $15.00 USD
Received 27 Dec 2012; accepted 5 Feb 2013; published 21 Mar 2013

positions for the simulated population of NCs, which is randomly variable with uniform distribution in the range $[0, \Delta R]$.

Results for the dipolar and higher order multipole scattering efficiencies are aggregated into the statistics shown in Fig. 13. Solid lines representing the scattering efficiencies for the nominal icosahedral NC configuration are plotted as references. It can be observed that the considered random displacement of nanosatellites from their nominal positions weakly influences the positions and strengths of NC collective resonance. In particular, the effect of positional disorder appears to be much less important than that of dimensional disorder for comparable maximum deviations from the nominal parameter values. Indeed, the variances of the scattering efficiencies for positional disorder are rather small. Even the generally more sensitive magnetic resonance (the peak of $Q_{sca}^{p_m}$) is very stable with respect the statistical variations of the nanosphere positions.

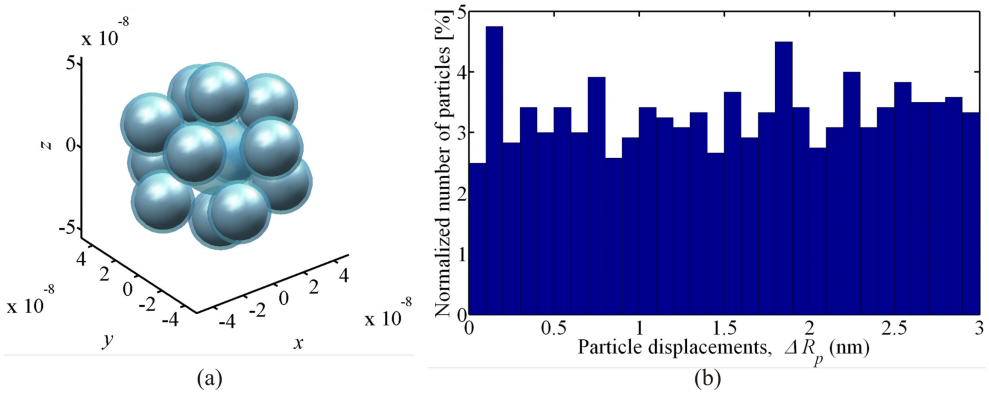

(a) (b)

Fig. 12. (a) Sample icosahedral NC with randomly variable particle positions ($r_0 = 15$, $\Delta R = 3$ nm). (b) Distribution of nanoparticle displacement distances from their nominal positions for the simulated population of 100 NCs.

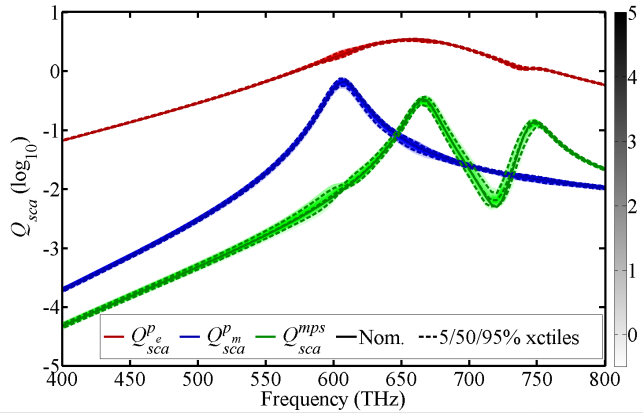

Fig. 13. Statistics of the scattering efficiency contributions associated with the induced electric and magnetic dipole moments and the remaining higher order multipoles for the population of 100 icosahedral NCs with $r_0 = 15$ nm and variable nanosatellites positions ($\Delta R = 3$ nm) from Fig. 12. The 5, 50, and 95 percentile curves are superimposed to the relative empirical pdfs (color shaded stripes).

#182380 - $15.00 USD
Received 27 Dec 2012; accepted 5 Feb 2013; published 21 Mar 2013

4.3 NC made of 32 plasmonic nanosatellites

As another example we consider the 32-element NC with nanoparticle of radius 10 nm arranged around a central dielectric core of radius $a = 31.7$ nm, with overall size of the NC $D = 111.4$ nm. The surface-to-surface distance between two nanosatellites in the nominal configuration is $d_p = 8$ nm. In this case we assume a maximum displacement distance from nanoparticle nominal positions $\Delta R = 2$. Figure 14 shows an instance of the simulated population of 32-element NCs (Fig. 14(a)), and the distribution of nanoparticle displacement distances from their nominal positions (Fig. 14(b)). The statistics for the simulated scattering efficiencies of the 32-element NC population are plotted in Fig. 15. The two main observations that can be discerned from this plot are that, similarly to the Platonic NCs analyzed previously (the tetrahedral and icosahedral NCs), the effect of particle position disorder is less important that variability of particle size. Moreover, for the same relative amount of positional disorder ($\Delta R / r_0$), the optical response of NCs comprising a larger number of particles turns out to be less perturbed by the randomness of particle positions. Indeed, we can observe in Fig. 15 that positions and strengths of NC collective resonance are insubstantially affected by the introduction of positional disorder, and variances of the scattering efficiencies are practically negligible.

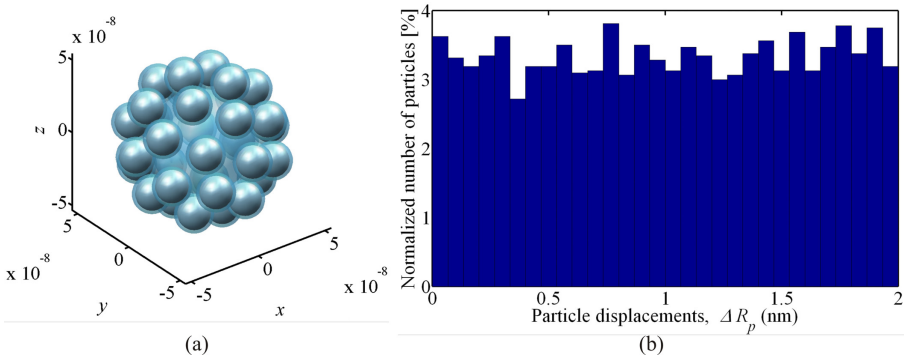

(a) (b)

Fig. 14. (a) Sample 32-element NC with randomly variable particle positions ($r_0 = 10$, $\Delta R = 2$ nm). (b) Distribution of nanoparticle displacement distances from their nominal positions for the simulated population of 100 NCs.

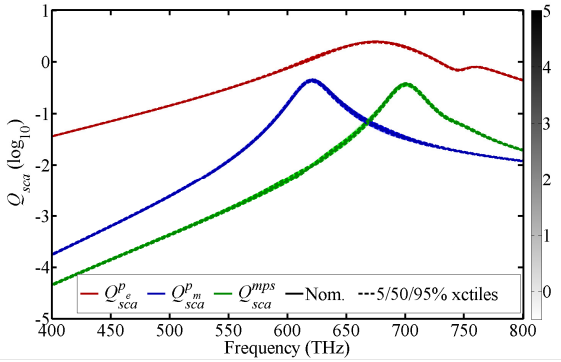

Fig. 15. Statistics of the scattering efficiency contributions associated with the induced electric and magnetic dipole moments and the remaining higher order multipoles for the population of 32-nanosatellites NCs with $r_0 = 10$ nm and variable nanosatellites positions ($\Delta R = 2$) nm from Fig. 14. The 5, 50, and 95 percentile curves are superimposed to the relative empirical pdfs (color shaded stripes).

#182380 - $15.00 USD Received 27 Dec 2012; accepted 5 Feb 2013; published 21 Mar 2013

4.4 NC made of 48 plasmonic nanosatellites

Finally, we have examined the effects of disordered particle positions in the 48-element NC considered previously in Fig. 8, with silver nanosatellites of radius $r_0 = 8.5$ nm attached to a central silica core of radius $a = 33.8$ nm, and an overall size of the NC $D = 116.4$ nm. We assume uniform particle radii and variable particle positions, with a maximum displacement distance from nanoparticle nominal positions $\Delta R = 1.7$. The surface-to-surface distance between two nanoparticles in the nominal configuration is 7.4 nm. Figure 16 shows an instance of the simulated population of 48-element NCs (Fig. 16(a)), and the distribution of nanoparticle displacement distances from their nominal positions (Fig. 16(b)). The statistics for the simulated scattering efficiencies of the 48-element NC population are plotted in Fig. 17. As for the NC configurations analyzed previously, the effect of particle position disorder is less important than that of variability of particle size. Moreover, for the same relative amount of positional disorder ($\Delta R / r_0$), the optical response of NCs comprising a larger number of satellites turns out to be practically insensitive to randomness of particle positions.

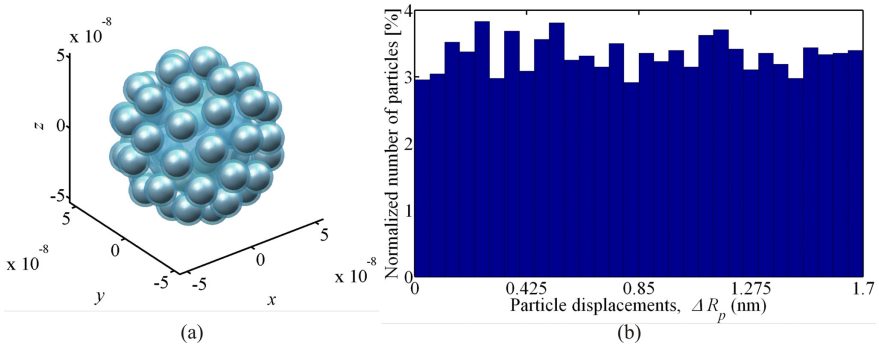

(a) (b)

Fig. 16. (a) Sample 48-element NC with randomly variable particle positions ($r_0 = 8.5$, $\Delta R = 1.7$ nm). (b) Distribution of nanoparticle displacement distances from their nominal positions for the simulated population of 100 NCs.

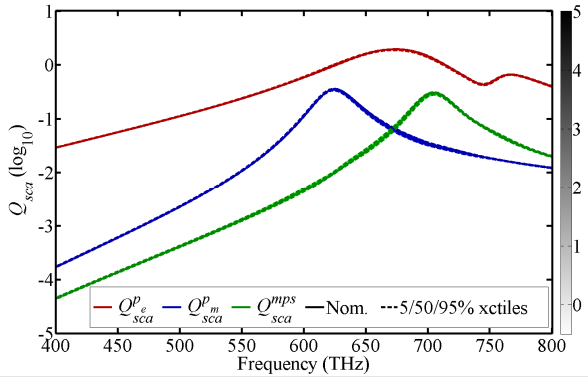

Fig. 17. Statistics of the scattering efficiency contributions associated with the induced electric and magnetic dipole moments and the remaining higher order multipoles for the population of 48-nanosatellites NCs with $r_0 = 8.5$ nm and variable nanosatellites positions ($\Delta R = 1.7$ nm) from Fig. 16. The 5, 50, and 95 percentile curves are superimposed to the relative empirical pdfs (color shaded stripes).

#182380 - $15.00 USD
Received 27 Dec 2012; accepted 5 Feb 2013; published 21 Mar 2013

5. Effect of nanosatellites defects on nanocluster response

In this section we analyse the effects of the presence of satellites defects in the NCs that may occur because particles can physically block one another in the process of self-assembly around the silica core. Defects are introduced by removing a number of nanosatellites at random locations from the ordered and complete NC configurations. We consider the same reference NC configurations examined in the previous sections, that is the tetrahedral, icosahedral, and the semiregular 32- and 48-element NCs, with the same nominal geometrical dimensions of the metallic nanosatellites and dielectric core as specified above. For all the considered types of NCs, we remove a subset of (possibly adjacent) nanoparticles corresponding to the 25% of the total number of constituent particles, i.e., 1, 4, 8, and 12 nanosatellites for the tetrahedral, icosahedral, 32- and 48-element NCs, respectively.

Except that for the tetrahedral NC, for which introduction of a single defect leads to only 4 possible different configurations, for all the other types of NCs we randomly select a population of 100 NCs from all the possible configurations with the specified number of defects at different sets of locations. After computing by the SDA the individual scattering responses of the NC population for illumination by a linearly polarized plane wave, we aggregate statistically the results obtained for the scattering efficiencies of the different types of defective NCs (except that for the tetrahedral NCs whose population comprises only four instances). It has to be noted that in our analysis we computed the scattering efficiencies by choosing specific z propagating plane wave illumination with electric field along x and magnetic field along y. While the nominal NCs were demonstrated to be highly isotropic because of symmetry [6], thus rendering the scattering efficiency value practically independent of the particular plane wave direction, the defective NCs might become not symmetric and therefore their response might be significantly affected by the impinging plane wave direction. However, the collection of different defective NCs used for the statistical analysis also comprises individual which differs for a spatial rotation; therefore such an analysis is also representative of the dependence of the scattering efficiency on the direction of illumination and reveals the degree of isotropy exhibited by the defective NCs.

5.1 NC made of 4 plasmonic nanosatellites

Figure 18(a) shows one of the defective tetrahedral NCs with one missing particle, and the results for the scattering efficiencies of the set of 4 tetrahedral NCs with one defects are plotted in Fig. 18(b). As apparent, the removal of a single nanoparticle completely disrupts the symmetry of this type of NCs and their response to a given incident polarization strongly depends on the specific NC configuration and the location of the missing particle: for one of the defective tetrahedral NCs both the electric and magnetic resonance almost disappear, for another NC resonances are practically unaffected, and for the remaining two configurations the electric resonance is substantially preserved, while the magnetic resonance is shifted to higher frequency or attenuated to the level of the higher order multipole contribution.

#182380 - $15.00 USD Received 27 Dec 2012; accepted 5 Feb 2013; published 21 Mar 2013

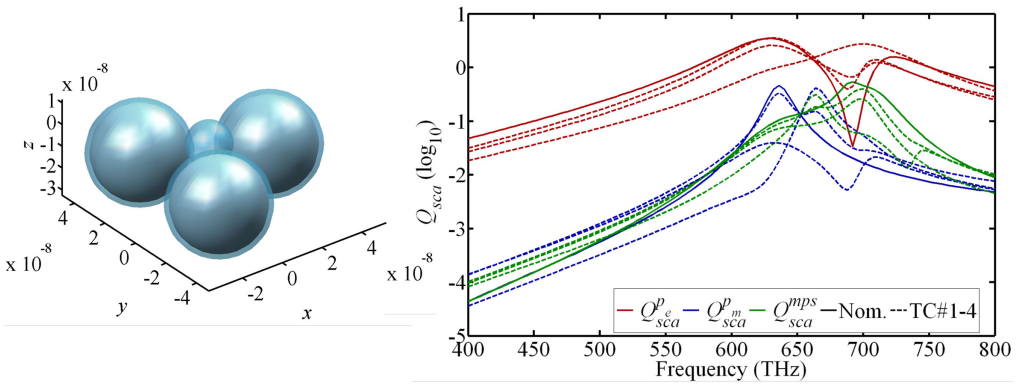

(a) (b)

Fig. 18. (a) Sample defective tetrahedral NC ($r_0 = 20$ nm) with 1 missing nanosatellite. (b) Scattering efficiency contributions associated with the induced electric and magnetic dipole moments and the remaining higher order multipoles of the four tetrahedral NCs with 1 defect.

5.2 NC made of 12 plasmonic nanosatellites

A sample defective icosahedral NC with 3 missing particles is shown in Fig. 19(a). Results for the dipolar and higher order multipole scattering efficiencies for the selected population of 100 defective icosahedral NCs are aggregated into the statistics shown in Fig. 19(b) in comparison with the corresponding efficiencies for the nominal NC configuration (solid lines). The impact of the presence of defects on the response of the icosahedral NCs is less dramatic than in the tetrahedral NCs but is still noticeable. It can be observed that for the defective NCs the magnetic resonance is shifted to higher frequencies with respect to the reference NC and its amplitude undergoes significant variations across the NC population. The presence of defects also produces a significant dispersion of the electric dipole scattering efficiencies, but their median values (50 percentile) are closer to the corresponding reference curve and no shift of the resonance frequency is observed. These trends can be interpreted in light of the NC resonance phenomenology outlined in [6]. The electric resonance, for a given separation between the particles, is essentially related to the size of a single particle and its strength to the number of constituent particles and the interaction effects among them, which obviously are stronger at the particle resonance. Since the incident field direction is fixed, locations of defects can significantly affect the electric resonance amplitude. Instead, the magnetic mode is supported by currents circulating around the central dielectric core of the cluster, and its resonance depends on the size of this current loop and on the distance between contiguous nanospheres in the plasmonic nanorings. In the defective configurations, missing particles determine a reduction of the NC equivalent inductance, while the larger gaps between the nanoparticles decrease the total capacitance of the nanoring; accordingly the magnetic resonance inevitably shifts to higher frequencies, though its strength is less sensitive to the locations of defects.

#182380 - $15.00 USD Received 27 Dec 2012; accepted 5 Feb 2013; published 21 Mar 2013

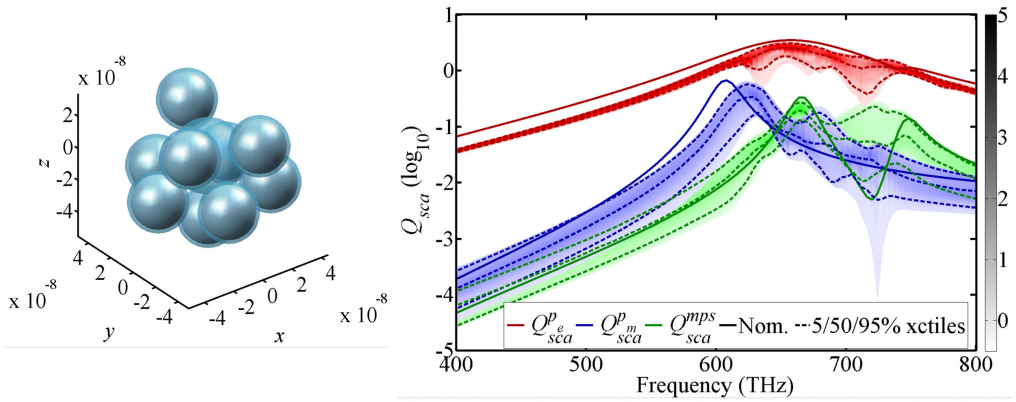

(a) (b)

Fig. 19. (a) Sample defective icosahedral NC ($r_0 = 15$) with 3 missing nanosatellites. (b) Statistics of the scattering efficiency contributions associated with the induced electric and magnetic dipole moments and the remaining higher order multipoles for the population of 100 defective icosahedral NCs with variable locations of the 3 missing nanosatellites. The 5, 50, and 95 percentile curves are superimposed to the relative pdfs (color shaded stripes).

5.3 NC made of 32 plasmonic nanosatellites

From the 32-element NC we remove 8 particles, as in the sample defective NC depicted in Fig. 19(a). The statistics for the simulated scattering efficiencies of the population of 32-element NCs with 8 defects are plotted in Fig. 19(b).

It appears that for this type of NC the shift of the magnetic resonance, which is associated with the reduction of the cluster capacitance and inductance as explained above, is less pronounced than in the populations of defective tetrahedral and icosahedral NCs previously analyzed. Moreover, the variability of the locations of missing particles across the NC population determines smaller fluctuations of the electric and magnetic responses.

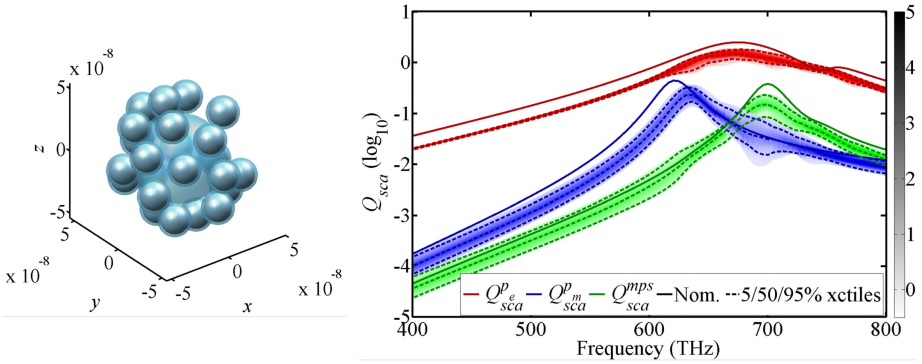

(a) (b)

Fig. 20. (a) Sample defective 32-element NC ($r_0 = 10$ nm) with 8 missing nanosatellites. (b) Statistics of the scattering efficiency contributions associated with the induced electric and magnetic dipole moments and the remaining higher order multipoles for the population of defective 32-element NCs with variable locations of the 8 missing nanosatellites. The 5, 50, and 95 percentile curves are superimposed to the relative empirical pdfs (color shaded stripes).

5.4 NC made of 48 plasmonic nanosatellites

A sample of a defective 48-element NC after removal of a subset of 12 nanosatellites is shown in Fig. 20(a). Simulated results for the scattering efficiencies of a population of 100 of

#182380 - $15.00 USD
Received 27 Dec 2012; accepted 5 Feb 2013; published 21 Mar 2013

these defective NCs are aggregated into the statistics shown in Fig. 20(b). The observations made above for the defective 32-element NCs apply a fortiori to the defective 48-element NCs. The shift of the magnetic resonance is further reduced as well as the variances of the electric and magnetic scattering responses associated with the random locations of the missing nanosatellites across the NC population.

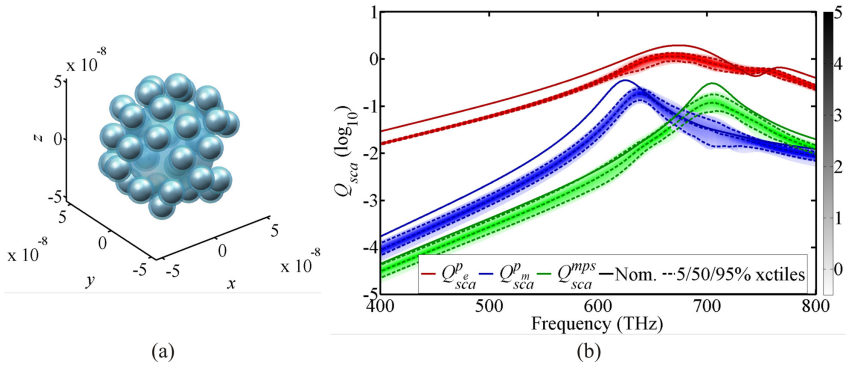

(a) (b)

Fig. 21. (a) Sample defective 48-element NC (r_0 = 8.5 nm) with 12 missing nanosatellites. (b) Statistics of the scattering efficiency contributions associated with the induced electric and magnetic dipole moments and the remaining higher order multipoles for the population of defective 48-element NCs with variable locations of the 12 missing nanosatellites. The 5, 50, and 95 percentile curves are superimposed to the relative empirical pdfs (color shaded stripes).

6. Conclusion

We have investigated the optical response of 3D NCs exhibiting some degree of dimensional or positional disorder at the level of the constituent metal nanoparticles or presenting defects, i.e. with a number of missing nanoparticles, by Monte Carlo simulations. In all cases the magnetic resonance is more sensitive to the statistical variations than the electric resonance. We have shown that displacement of nanoparticles from their nominal positions does not significantly impact the optical response of NCs, whereas variability of particle sizes and the presence of defects reduce the intensity of the average electric and magnetic responses and can also determine a displacement of the magnetic resonance frequency. In addition, the resulting large variance of the response around the average value, for the various NCs in the population, reveals a degradation of the isotropicity with respect to the nominal NC as a result of the lack of symmetry. At any rate, obtained results shown that NCs comprising a larger number of particles can be more insensitive to the effects of disorder and the presence of defects. The counterpart for the substantial immunity to various types of irregularities exhibited by the NCs comprising a larger number of nanosatellites is a reduction of the intensity of the electric and magnetic responses, as a consequence of the increased absorption occurring in the smaller size nanosatellites. However, for the considered NCs such reduction of scattering efficiencies is limited and the magnetic resonance, which is more affected than the electric one, is always present. We believe that the observed trends are important and can serve as guidelines for the design of NCs exhibiting the desired optical properties.

Acknowledgments

The authors acknowledge partial support from the European Commission 7th Framework Program FP7/2008, “Nanosciences, Nanotechnologies, Materials and New Production Technologies (NMP)” theme, research area “NMP-2008-2.2-2 Nanostructured meta-materials”, grant agreement number n° 228762. F.C. acknowledges partial support from the National Science Foundation (NSF)-CMMI award 1101074.